spectrometer. The observing frequencies were 250.161 (^{1}H), 47.704 (^{77}Se), and 78.917 MHz (^{125}Te) on the WM-250 spectrometer and 500.138 (^{1}H), 95.383 (^{77}Se), 130.885 (^{123}Te), and 157.792 MHz (^{125}Te) on the AM-500 spectrometer. Free induction decays were typically accumulated in 16 K or 32K memories. Spectral width settings of 25-100 kHz were employed, yielding data point resolutions of 3.0-6.1 Hz and acquisition times of 0.328-0.655 s, respectively. No relaxation delays were applied. The number of free induction decays accumulated depended upon the concentration and sensitivity of the nucleus under consideration with 10 000-300 000 scans being typical for these samples. Pulse widths for bulk magnetization tip angles corresponding to 90° were 2 (^{1}H), 20 (^{77}Se), and 25 μs (^{125}Te) on the WM-250 spectrometer and 2 (^{1}H), 12 (^{77}Se), 26 (^{123}Te), and 10-18 μs (^{125}Te) on the AM-500 spectrometer. Line-broadening parameters used in the exponential multiplication of the free-induction decays were 5-20 Hz for the heavier isotopes; however, values on the order of 100-350 Hz were used for the broad lines. In order to enhance the resolution of some satellite peaks, the free induction decay was transformed with the use of a Gaussian fit rather than the conventional Lorentzian fit. In these instances, Gaussian broadenings of between 0.1 and 0.5 Hz and a line broadening greater than or equal to the negative of the data point resolution were applied.

The respective nuclei were referenced to neat samples of $(CH_3)_2Se$ (^{77}Se), $(CH_3)_2Te$ (^{123}Te and ^{125}Te), and $(CH_3)_4Si$ (^{1}H) at 24 °C. The chemical shift convention used is that a positive (negative) sign signifies a chemical shift to high (low) frequency of the reference compound.

Acknowledgment. We wish to thank the Natural Sciences and Engineering Research Council of Canada for support of this work and McMaster University and the Ontario Ministry of Colleges and Universities for the award of scholarships to M.B.

Contribution from the Department of Chemistry, University of California, Davis, California 95616

Three-Coordinate Iron Complexes: X-ray Structural Characterization of the Amide-Bridged Dimers $[Fe(NR_2)_2]_2$ (R = $SiMe_3$, C_6H_5) and the Adduct $Fe[N(SiMe_3)_2]_2(THF)$ and Determination of the Association Energy of the Monomer $Fe\{N(SiMe_3)_2\}_2$ in Solution

Marilyn M. Olmstead, Philip P. Power,* and Steven C. Shoner

Received November 12, 1990

The X-ray structural characterization of the iron(II) amides $[Fe\{N(SiMe_3)_2\}_2]_2$ (**1**) and $[Fe(NPh_2)_2]_2$ (**2**) and the Lewis base adduct $Fe[N(SiMe_3)_2]_2(THF)$ (**3**), as well as the syntheses of the last two compounds, is described. These complexes are rare examples of the coordination number 3 for iron. Compounds **1** and **2** are both dimeric in the solid state, with each trigonal-planar ion bound to one terminal and two bridging amides. They closely resemble the corresponding Mn(II) and Co(II) compounds. Compound **3** is monomeric in the solid state, with one THF and two amides arranged in a trigonal-planar fashion. The terminal Fe-N bond lengths in **1**-**3** are similar to those reported for two-coordinate iron(II) amides. The Fe-N bonds in **1** are somewhat longer than those in **2**, indicating weaker association in **1**. This is borne out in the solution behavior of the two compounds. Thus **1**, which was studied by variable-temperature ^{1}H NMR spectroscopy, was seen to be a monomer in solution at 30 °C. Increasing amounts of the dimer were observed at lower temperature, and calculations based on the monomer-dimer equilibrium indicate an association energy of ~+3 kcal mol^{-1} for $[Fe\{N(SiMe_3)_2\}_2]_2$. Crystal data with Mo Kα (λ = 0.71069 Å) radiation at 130 K: **1**, $C_{24}H_{72}Fe_2N_4Si_8$, a = 17.978 (4) Å, b = 14.691 (4) Å, c = 18.564 (5) Å, β = 120.15 (2)°, Z = 4, monoclinic, space group $C2/c$, R = 0.031; **2**, $C_{48}H_{40}Fe_2N_4$, a = 9.579 (5) Å, b = 10.264 (5) Å, c = 10.482 (6) Å, α = 91.78 (4)°, β = 110.68 (4)°, γ = 85.67 (4)°, Z = 1, triclinic space group $P\bar{1}$, R = 0.039; **3**, $C_{16}H_{44}FeN_2OSi_4$, a = 11.225 (5) Å, b = 13.391 (5) Å, c = 17.903 (8) Å, Z = 4, orthorhombic, space group $Pcan$, R = 0.061.

Introduction

The use of bulky amide ligands to synthesize low-coordinate transition-metal complexes originated with two seminal[1,2] papers in the early 1960s that described the use of the $-N(SiMe_3)_2$ group to synthesize transition-metal compounds of the formula $M[N(SiMe_3)_2]_n$ (M = Cu[2] n = 1; M = Mn,[2] Co,[1] Ni,[2] n = 2; M = Cr,[2] Fe,[1] n = 3). This work was later extended to include further tris(amido) derivatives $M[N(SiMe_3)_2]_3$ (M = Sc, Ti, or V[3] and the lanthanides[4]). In addition, their chemistry and some aspects of the chemistry of the divalent transition-metal[3,5,6] and lanthanide amides[7] were explored. Structural data have appeared for many of these, including $[M\{N(SiMe_3)_2\}_2]_2$ (M = Mn,[8,9] Co[9]) and, in addition, the three-coordinate Lewis base adducts $Mn[N(SiMe_3)_2]_2(THF)$,[5] $Co[N(SiMe_3)_2]_2(PPh_3)$,[6] and $M[N(SiMe_3)_2](PPh_3)_2$ (M = Co, Ni).[6] Many of these compounds were among the earliest well-characterized three-coordinate transition-metal complexes. Until recently, hardly any data had appeared on iron(II) amides.[10,11] The synthesis of $Fe[N(SiMe_3)_2]_2$[11] was not reported until 1988, and it was shown that both it and its manganese and cobalt analogues were two-coordinate in the gas phase by electron diffraction. Magnetic data and PES data for all three compounds were also reported.[11]

Investigation of transition-metal amides in this laboratory stems in part from a general interest in the structures and reactivity of

(1) Bürger, H.; Wannagat, U. *Monatsh. Chem.* **1963**, *94*, 1007.
(2) Bürger, H.; Wannagat, U. *Monatsh. Chem.* **1964**, *95*, 1099.
(3) Bradley, D. C. *Chem. Br.* **1975**, *11*, 353. Alyea, E. C.; Bradley, D. C.; Copperthwaite, R. G. *J. Chem. Soc., Dalton Trans.* **1972**, 1580.
(4) Bradley, D. C.; Ghotra, J. S.; Hursthouse, M. B.; Welch, A. J. *J. Chem. Soc., Chem. Commun.* **1973**, 669. Bradley, D. C.; Ghotra, J. S.; Hart, F. A.; Hursthourse, M. B.; Raithby, P. R. *J. Chem. Soc., Dalton Trans.* **1977**, 1166.
(5) Eller, P. G.; Bradley, D. C.; Hursthouse, M. B.; Meek, D. W. *Coord. Chem. Rev.* **1977**, *24*, 1.
(6) Bradley, D. C.; Hursthouse, M. B.; Newing, C. W.; Welch, A. J. *J. Chem. Soc., Chem. Commun.* **1972**, 567. Bradley, D. C.; Hursthouse, M. B.; Smallwood, R. J.; Welch, A. J. *J. Chem. Soc., Chem. Commun.* **1972**, 872.
(7) Tilley, T. D.; Andersen, R. A. *J. Chem. Soc., Chem. Commun.* **1981**, 985; *J. Am. Chem. Soc.* **1982**, *104*, 1172. Tilley, T. D.; Andersen, R. A.; Zalkin, A. *Inorg. Chem.* **1984**, *23*, 2271.
(8) Bradley, D. C.; Hursthouse, M. B.; Malik, K. M. A.; Moseler, R. *Transition Met. Chem. (London)* **1978**, *3*, 253.
(9) Murray, B. D.; Power, P. P. *Inorg. Chem.* **1984**, *23*, 4584.
(10) Bartlett, R. A.; Power, P. P. *J. Am. Chem. Soc.* **1987**, *109*, 7563.
(11) Andersen, R. A.; Faegri, K.; Green, J. C.; Haaland, A.; Lappert, M. F.; Leung, W.-P. *Inorg. Chem.* **1988**, *27*, 1782.

0020-1669/91/1330-2547$02.50/0

Table I. Abridged Summary of Data Collection, Structure Solution, and Refinement for **1–3**[a]

	1	2	3
formula	$C_{24}H_{72}Fe_2N_4Si_8$	$C_{48}H_{40}Fe_2N_4$	$C_{16}H_{44}FeN_2OSi_4$
fw	753.90	784.57	448.90
cryst syst	monoclinic	triclinic	orthorhombic
a, Å	17.978 (4)	9.579 (5)	11.225 (5)
b, Å	14.691 (4)	10.264 (5)	13.391 (5)
c, Å	18.564 (5)	10.482 (6)	17.903 (8)
α, deg		91.78 (4)	
β, deg	120.15 (2)	110.68 (4)	
γ, deg		85.67 (4)	
V, Å	4240 (2)	961.5 (8)	2691.1 (2)
space group	$C2/c$	$P\bar{1}$	*Pcan* (*bac* of *Pbcn*, No. 60)
Z	4	1	4
d_{calc}, g cm^{-3}	1.18	1.35	1.11
linear abs coeff, cm^{-1}	9.26	7.92	7.4
2θ range, deg	0–50	0–50	0–50
no. of obs reflcns	2985 [$I > 2\sigma(I)$]	2735 [$I > 2\sigma(I)$]	1443 [$I > 2\sigma(I)$]
no. of variables	210	244	128
R, R_w	0.031, 0.032	0.039, 0.038	0.061, 0.063

[a] Data were collected at 130 K with Mo Kα radiation (λ = 0.710 69 Å.

two-coordinate transition-metal complexes. Recent work has shown that the bulky silylamides $-N(SiMePh_2)_2$ and $-N(SiMe_2Ph)_2$[10,12] and the borylamides $-NRBMes_2$ (R = Ph, Mes)[13,14] allowed the isolation and structural characterization of two-coordinate crystalline complexes of several first-row (Cr → Ni) transition metals.[15] In addition, reports on the structures and properties of the divalent amides $[M\{N(SiMe_3)_2\}_2]_2$ (M = Mn, Co)[8,9] and $[M(NPh_2)_2]_2$ (M = Co, Ni)[15,16] have appeared. The silylamides $M[N(SiMe_3)_2]_2$ (M = Mn, Fe, Co), which in the case of Co[17] and Fe are two-coordinate in solution, have proven to be excellent starting materials for the higher valent amides $M[N(SiMe_3)_2]_3$[18] (M = Mn, Co), divalent phosphides and arsenides,[19] and low-coordinate divalent alkoxides $[M(OAr)_2]_2$ (M = Mn, Fe)[20] and thiolates $[M(SAr)_2]_2$ (M = Mn, Fe, Co, Ar = 2,4,6-t-$Bu_3C_6H_2$).[21] As part of these studies, we report here on the X-ray crystal structures of $[Fe(NR_2)_2]_2$ (R = $SiMe_3$ (**1**), Ph (**2**)), and the Lewis base adduct $Fe[N(SiMe_3)_2]_2(THF)$ (**3**) and a temperature-dependent, dynamic ^1H NMR study of the solution behavior of **1**. The crystal structures of the title compounds have been mentioned briefly in a recent review.[15]

Experimental Section

General Procedures. All reactions were performed under N_2 by using either modified Schlenk techniques or a Vacuum Atmospheres HE 43-2 drybox. Solvents were freshly distilled from Na/K and degassed three times before use. $FeBr_2$, $HN(SiMe_3)_2$, and $HNPh_2$ were purchased from common sources and used as received. $[Fe\{N(SiMe_3)_2\}_2]_2$ (**1**) was prepared by the literature procedure.[11] ^1H NMR spectra were recorded in C_7D_8 at 300 MHz on a GE QE-300 spectrometer.

Synthesis of $[Fe(NPh_2)_2]_2$ (2). A 6.25-mL portion of a 1.6 M n-BuLi solution in hexane was added dropwise to 1.69 g (10 mmol) of $HNPh_2$ in THF (60 mL) with cooling in an ice bath. Stirring was continued for 1 h. $FeBr_2$, 1.08 g (5 mmol), was added via a solid-addition funnel. The solution turned dark red-green and was allowed to warm to room temperature and stir overnight. The volatiles were removed under reduced pressure, leaving a black-red residue. The residue was extracted several times with 30 mL of hot toluene, and the extract was filtered. On cooling to room temperature, the dark red solution yielded dark red crystals of **2**.

$Fe[N(SiMe_3)_2]_2(THF)$ (3). A solution of $LiN(SiMe_3)_2$ (30 mmol) in THF (40 mL), synthesized from $HN(SiMe_3)_2$ (4.8 g, 30 mL) and 18.75 mL of a 1.6 M n-BuLi solution in hexane, was added dropwise to $FeBr_2$ (3.24 g, 15 mmol) in THF (20 mL) with cooling in an ice bath. Stirring was continued overnight at room temperature to give a green-brown solution. The volatile material was removed under reduced pressure. Redissolving in hexane (30 mL), filtration, and immediate distillation (80 °C/0.2 mmHg) afforded the product **3** as a pale green oil. Yield: 6.1 g, 91%. The oil solidified upon standing to give the product as pale green crystals that were suitable for X-ray crystallography.

X-ray Crystallographic Studies. All X-ray data were collected with a Syntex $P2_1$ diffractometer equipped with a locally modified LT-1 low-temperature device. All calculations were carried out on a Data General Eclipse computer using the SHELXTL, Version 5, program system. Scattering factors were from common sources.[22] An absorption correction was applied by using the method described in ref 22.

Green crystals of **1** and **3** were grown over several days from melts of the compounds that had been freshly distilled. Red needles of **2** were grown by slow cooling to room temperature of a solution of the compound in hot toluene. The crystals were removed from a Schlenk tube under a stream of N_2 and immediately covered with a layer of hydrocarbon oil. A suitable crystal was selected, attached with grease to a glass fiber, and

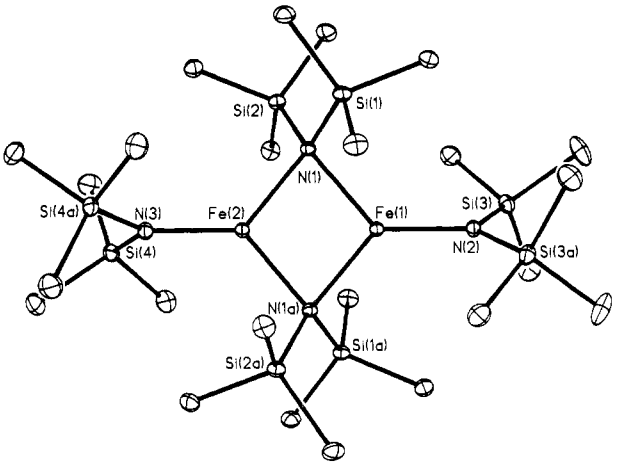

Figure 1. Thermal ellipsoid drawing of $[Fe\{N(SiMe_3)_2\}_2]_2$ (**1**). The H atoms are omitted for clarity. N(1) and N(1a) are related by a 2-fold axis along the Fe(1)···Fe(2) vector.

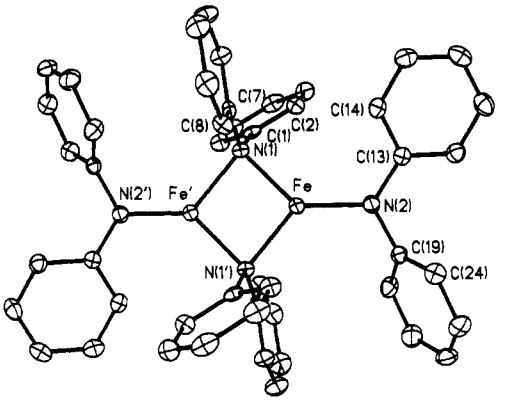

Figure 2. Thermal ellipsoid drawing of $[Fe(NPh_2)_2]_2$ (**2**). The H atoms are omitted for clarity. Fe and Fe' are related by an inversion center.

(12) Chen, H.; Bartlett, R. A.; Dias, H. V. R.; Olmstead, M. M.; Power, P. P. *J. Am. Chem. Soc.* **1989**, *111*, 4338.
(13) Bartlett, R. A.; Feng, X.; Olmstead, M. M.; Power, P. P.; Weese, K. J. *J. Am. Chem. Soc.* **1987**, *109*, 4851.
(14) Chen, H.; Bartlett, R. A.; Olmstead, M. M.; Power, P. P.; Shoner, S. C. *J. Am. Chem. Soc.* **1990**, *112*, 1048.
(15) Power, P. P. *Comments Inorg. Chem.* **1989**, *8*, 177.
(16) Hope, H.; Olmstead, M. M.; Murray, B. D.; Power, P. P. *J. Am. Chem. Soc.* **1985**, *107*, 712.
(17) Bradley, D. C.; Fisher, K. J. *J. Am. Chem. Soc.* **1971**, *93*, 921.
(18) Ellison, J. J.; Power, P. P.; Shoner, S. C. *J. Am. Chem. Soc.* **1989**, *111*, 8044.
(19) Chen, H.; Olmstead, M. M.; Pestana, D. C.; Power, P. P. *Inorg. Chem.* **1991**, *30*, 1783.
(20) Bartlett, R. A.; Ellison, J. J.; Shoner, S. C.; Power, P. P. *Inorg. Chem.*, in press.
(21) Shoner, S. C.; Power, P. P. *Angew. Chem., Int. Ed. Engl.* **1991**, *30*, 330.
(22) *International Tables for X-Ray Crystallography*; Kynoch Press: Birmingham, U.K., 1974; Vol. IV. The absorption correction was made by using the Program XABS. The program obtains an absorption tensor from $F_o - F_c$ differences: Moezzi, B. Ph.D. Dissertation, University of California, Davis, 1987.

Table II. Selected Atomic Coordinates (×10⁴) and Isotropic Thermal Parameters (Å² × 10³) for **1–3**

	x	*y*	*z*	*U*[a]
		$[Fe\{N(SiMe_3)_2\}_2]_2$ (**1**)		
Fe(1)	5000	1513 (1)	2500	14 (1)
Fe(2)	5000	3326 (1)	2500	14 (1)
Si(1)	6789 (1)	1983 (1)	2900 (1)	17 (1)
Si(2)	5606 (1)	2857 (1)	1283 (1)	18 (1)
Si(3)	4581 (1)	−388 (1)	1569 (1)	22 (1)
Si(4)	4140 (1)	5234 (1)	1720 (1)	23 (1)
N(1)	5725 (1)	2421 (1)	2238 (1)	14 (1)
N(2)	5000	201 (2)	2500	18 (1)
N(3)	5000	4635 (2)	2500	20 (1)
		$[Fe(NPh_2)_2]_2$ (**2**)		
Fe	607 (1)	1138 (1)	4934 (1)	17 (1)
N(1)	19 (2)	364 (2)	6422 (2)	14 (1)
N(2)	1657 (3)	2594 (2)	4810 (2)	19 (1)
C(1)	−1184 (3)	1211 (3)	6602 (3)	16 (1)
C(7)	1226 (3)	−38 (5)	7645 (3)	15 (1)
C(13)	2341 (3)	3431 (3)	5909 (3)	17 (1)
C(19)	1607 (3)	2930 (3)	3487 (3)	18 (1)
		$Fe[N(SiMe_3)_2]_2(THF)$ (**3**)		
Fe	3352 (1)	0	2500	34 (1)
Si(1)	3041 (4)	−1308 (1)	1080 (1)	44 (1)
Si(2)	2050 (2)	806 (2)	1113 (1)	56 (1)
N	2825 (4)	−174 (3)	1491 (3)	35 (2)
O	5197 (5)	0	2500	59 (2)
C(7)	5930 (6)	328 (7)	1888 (4)	81 (3)

[a] Equivalent isotropic *U* defined as one-third of the trace of the orthogonalized U_{ij} tensor.

immediately placed in the low-temperature nitrogen stream. Some details of the data collection and refinement are given in Table I. Further details are provided in the supplementary material.

The structures **2** and **3** were solved by direct methods and subsequently refined by blocked-cascade least-squares refinement. Hydrogen atoms were included by use of a riding model with C–H distances of 0.96 Å and isotropic thermal parameters equal to 1.2 times that of the bonded carbon. All non-hydrogen atoms were refined anisotropically. In the case of **1**, atomic positions were taken from the isostructural compound $[Mn\{N(SiMe_3)_2\}_2]_2$[8,9] and, with iron placed on the manganese position, refinement was carried out as described for **2** and **3**. Atomic coordinates for **1–3** are given in Table II, and selected bond distances and angles are given in Table III.

Results and Discussion

Structural Descriptions. $[Fe\{N(SiMe_3)_2\}_2]_2$ (1) and $[Fe(NPh_2)_2]_2$ (2). The structures of **1** and **2** are shown in Figures 1 and 2, respectively. These compounds have a dimeric structure with two bridging and two terminal amide groups such that the irons have trigonal-planar coordination. Compound **1** possesses a crystallographically imposed 2-fold axis of rotation along the Fe···Fe vector. In contrast, **2** has an inversion center in the middle of the Fe_2N_2 core. The terminal Fe–N bond lengths in **1** and **2** are 1.925 (3) Å (average) and 1.895 (3) Å. The corresponding bridging Fe–N distances average 2.086 (2) and 2.038 (2) Å. Within the cores, the Fe–N–Fe angles are 70.4 (1)° (**1**) and 83.6 (1)° (**2**). This results in a shorter Fe···Fe distance for **1**, 2.663 (1) vs 2.715 (1) Å for **2**. The tilt angle between the Fe_2N_2 cores and the planes at the bridging nitrogens is 64.3° for **1** and 88.4° for **2**. The corresponding interplanar angles for the terminal amide groups are 71.2° for **1** but only 13.6° in the case of **2**. The bridging and terminal Si–N–Si angles for **1** are 111.2 (1) and 119.6 (4)°. The N–Si bond lengths in the bridging amide group are 1.794 (2) and 1.734 (3) Å in the terminal ligand.

$Fe[N(SiMe_3)_2]_2(THF)$ (3). This compound is illustrated in Figure 3. The iron is coordinated by two amides and a THF ligand and has a trigonal-planar geometry. There is a crystallographically imposed 2-fold axis along the Fe–O bond. The Fe–N distance is 1.916 (5) Å, and the Fe–O bond length is 2.071 (6) Å. The N–Fe–N angle (144.0 (3)°) is much larger than the O–Fe–N angle (108.0 (1)°). The angle between the Fe and N planes is 67°, and the Si–N–Si angle is 125.8 (3)° with a Si–N bond length of 1.709 (5) Å.

Table III. Selected Bond Distances (Å) and Angles (deg) for **1–3**

		$[Fe\{N(SiMe_3)_2\}_2]_2$ (**1**)	
Fe(1)–N(1)	2.086 (2)	N(1)–Si(1)	1.794 (2)
Fe(2)–N(1)	2.083 (2)	N(1)–Si(2)	1.794 (2)
Fe(1)–N(2)	1.927 (3)	N(2)–Si(3)	1.732 (2)
Fe(2)–N(3)	1.923 (3)	N(3)–Si(4)	1.735 (2)
N(1)–Fe(1)–N(1)′	100.5 (1)	Fe(2)–N(1)–Si(1)	130.2 (1)
N(1)–Fe(1)–N(2)	129.7 (1)	Fe(2)–N(1)–Si(2)	103.0 (1)
N(1)–Fe(2)–N(1)′	100.7 (1)	Si(1)–N(1)–Si(2)	111.2 (1)
N(1)–Fe(2)–N(3)	129.6 (1)	Fe(1)–N(2)–Si(3)	120.0 (1)
Fe(1)–N(1)–Fe(2)	79.4 (1)	Si(3)–N(2)–Si(3)′	120.0 (2)
Fe(1)–N(1)–Si(1)	100.8 (1)	Fe(2)–N(3)–Si(4)	120.5 (1)
Fe(1)–N(1)–Si(2)	132.9 (1)	Si(4)–N(3)–Si(4)′	119.1 (2)
		$[Fe(NPh_2)_2]_2$ (**2**)	
Fe–N(1)	2.036 (3)	N(1)–C(7)	1.437 (3)
Fe–N(2)	1.895 (3)	N(2)–C(13)	1.409 (3)
Fe–N(1)′	2.039 (2)	N(2)–C(19)	1.424 (4)
N(1)–C(1)	1.453 (4)		
N(1)–Fe–N(1)′	96.5 (1)	C(1)–N(1)–C(7)	116.3 (2)
N(1)–Fe–N(2)	135.1 (1)	C(1)–N(1)–Fe′	116.3 (2)
N(2)–Fe–N(1)′	127.8 (1)	C(7)–N(1)–Fe′	112.1 (2)
Fe–N(1)–Fe′	83.6 (1)	Fe–N(2)–C(13)	124.3 (2)
Fe–N(1)–C(1)	108.1 (2)	Fe–N(2)–C(19)	117.0 (2)
Fe–N(1)–C(7)	116.3 (2)	C(13)–N(2)–C(10)	118.4 (2)
		$Fe[N(SiMe_3)_2]_2(THF)$ (**3**)	
Fe–N	1.916 (5)	N–Si(1)	1.704 (5)
Fe–O	2.071 (6)	N–Si(2)	1.713 (5)
N–Fe–O	108.0 (1)	Si(1)–N–Si(2)	125.8 (3)
N–Fe–N′	144.0 (3)	Fe–O–C(7)	124.9 (3)
Fe–N–Si(1)	118.1 (2)	C(7)–O–C(7)′	110.2 (7)
Fe–N–Si(2)	115.8 (2)		

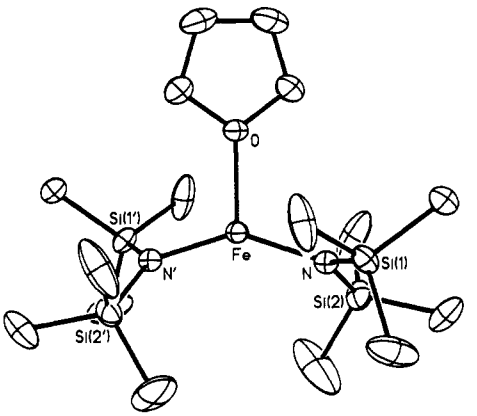

Figure 3. Thermal ellipsoid drawing of $Fe[N(SiMe_3)_2]_2(THF)$ (**3**). The H atoms are omitted for clarity. A 2-fold axis lies along the Fe–O bond.

Discussion

The title compounds were synthesized by the simple reactions

$$FeBr_2 + 2LiN(SiMe_3)_2 \xrightarrow{Et_2O} \underset{\mathbf{1}}{[Fe\{N(SiMe_3)_2\}_2]_2} + 2LiBr \quad (1)$$

$$FeBr_2 + 2LiNPh_2 \xrightarrow{THF} \underset{\mathbf{2}}{[Fe(NPh_2)_2]_2} + 2LiBr \quad (2)$$

$$FeBr_2 + 2LiN(SiMe_3)_2 \xrightarrow{THF} \underset{\mathbf{3}}{Fe[N(SiMe_3)_2]_2(THF)} + 2LiBr \quad (3)$$

in excellent yield (80–90%). Although the Mn and Co analogues of **1** have been known for over 25 years,[1,2] the synthesis of the Fe compound was reported only recently.[11] A possible reason for this was the apparent misconception[5] that attempts to prepare **1** always resulted in the isolation of $Fe[N(SiMe_3)_2]_3$. The high-yield syntheses of **1**,[11] $Fe[N(SiMe_2Ph)_2]_2$ (**4**),[12] and $Fe[N(SiMePh_2)_2]_2$ (**5**)[10,12] and the iron(II) amide complexes $Fe(NPh_2)_2(dioxane)_2$[23]

(23) Fröhlich, H.-O. *Z. Chem.* **1980**, *20*, 109.

Table IV. Selected Structural Data for Low-Coordinate Transition-Metal Amides (Distances, Å; Angles, deg)

	$[M\{N(SiMe_3)_2\}_2]_2$			$Fe[N(SiMe_3)_2]_2(THF)^b$	$Fe[N(SiMe_2Ph)_2]_2^d$	$Fe[N(SiMePh_2)_2]_2^{d,e}$
	M = Mn[a]	M = Fe[b] (1)	M = Co[a]	(3)	(4)	(5)
M···M	2.811 (1)	2.663 (1)	2.583 (3)			
M–N(t)	1.998 (3)	1.925 (3)	1.916 (5)	1.916 (5)	1.903 (7)	1.917 (2)
M–N(b)	2.174 (3)	2.085 (2)	2.061 (4)			
M–N–M	80.6 (1)	79.4 (1)	77.6 (2)			

	$[M(NPh_2)_2]_2$				
	M = Fe[b] (2)	M = Co[c]	M = Ni[c]	$Mn[N(SiMe_3)_2]_2(THF)^f$	$Fe[N(SiMe_3)_2]_2^g$ (6)
M···M	2.715 (1)	2.566 (3)	2.327 (2)		
M–N(t)	1.895 (3)	1.889 (8)	1.828 (9)	1.99 (2)	1.917 (3)
M–N(b)	2.038 (3)	1.998 (5)	1.911 (9)		
M–N–M	83.6 (1)	79.9 (3)	75.0 (3)		

Vapor Electron Diffraction Data[h] for $M[N(SiMe_3)_2]_2$

	M = Mn	M = Fe	M = Co
M–N	1.95 (2)	1.84 (2)	1.84 (2)

[a] References 8 and 9. [b] This work. [c] Reference 16. [d] Reference 10. [e] Reference 12. [f] Reference 5. [g] Reference 27. [h] Reference 11.

and $[Fe(NO)_2NPh_2]_2$[24] have shown this assumption to be false. The synthesis of the further examples, compounds **2** and **3**, has confirmed that low-coordinate iron(II) amides are just as readily synthesized as the other first-row transition-metal derivatives. A slight modification (replacement of Et_2O by THF solvent) of the synthesis of **1** resulted in the isolation of the THF adduct **3**, which can be distilled under reduced pressure without loss of the solvent molecule. The diphenylamido derivative **2** was also synthesized in excellent yield as indicated by eq 2. In this case, however, the use of THF as a solvent did not result in the formation of an adduct like **3**.

Although structurally similar, **1** and **2** exhibit different behavior in solution. For example, **1** is very soluble in all hydrocarbon solvents, whereas **2** is readily soluble only in hot toluene or in solvent mixtures involving more polar solvents (THF, Et_2O, etc.). Because of its low solubility, it is more difficult to study in solution. In contrast, **1** may easily be studied by ^1H NMR spectroscopy in either benzene or toluene.

Solution Behavior of $Fe[N(SiMe_3)_2]_2$. Several molecular weight determinations of **1** in PhMe by the Signer[25] method revealed molecular weight values not in excess of 400. This indicated that **1** is primarily monomeric in this solvent at ~27 °C. These data are supported by variable-temperature ^1H NMR studies. The ^1H NMR spectrum of **1** at 30 °C in C_7D_8 essentially shows only one broad peak at ~63 ppm. On cooling, two new peaks appear, one at 5.09 ppm and one much broader peak at −8.20 ppm. These new peaks intensify as the temperature is reduced further. By −50 °C the original downfield peak, which has shifted to ~84 ppm, almost disappears and only the two new peaks, now observed at 4.62 ppm and −7.82 ppm, remain. The single peak observed at room temperature at 63 ppm may be assigned to monomeric $Fe[N(SiMe_3)_2]_2$, since peaks at similar shifts, attributable to silicon–methyl groups, were observed at 50 and 57.6 ppm for the compounds $Fe[N(SiMe_2Ph)_2]_2$ (**4**) and $Fe[N(SiMePh_2)]_2$ (**5**), which are known to be monomeric in the crystalline phase.[10,12] Because **1** is monomeric, and because the shifts due to the $SiMe_3$ groups are similar to those previously observed in Fe^{2+} amide monomers, the single peak observed in the ^1H NMR spectrum may not be accounted for in terms of fast exchange between terminal and bridging groups of a dimer. Instead, the appearance of two peaks and the simultaneous disappearance of the original peak can be explained by the equilibrium

$$2Fe[N(SiMe_3)_2]_2 \rightleftarrows [Fe\{N(SiMe_3)_2\}_2]_2 \qquad (4)$$

Using the Van't Hoff equation over the range 283–233 K and the relative concentrations of monomer and dimer, derived from peak integration of a 0.12 M solution of **1**, to calculate the equilibrium constant gave a value of −19.4 kcal mol^{-1} for $\Delta H°_{reacn}$ and a value of −75.3 cal mol^{-1} K^{-1} for $\Delta S°_{reacn}$. At 300 K these figures lead to the conclusion that $\Delta G_{reacn} \approx +3$ kcal mol^{-1}. Clearly, the relatively large negative value for ΔS_{reacn} plays a key role in determining the position of the equilibrium for the weak association in eq 4. Thus, at 300 K the equilibrium constant, K, for eq 4 is 5×10^{-3} whereas at ~233 K it is ~60. In other words, at room temperature **1** is essentially (99.9%) monomeric but at −40 °C it is almost 80% associated. These data are in reasonable agreement with the molecular weight data for **1** in PhMe at room temperature. The data are also in harmony with earlier studies of the molecular weight of $Co[N(SiMe_3)_2]_2$[16] in cyclohexane and the monomeric character of $M[N(SiMe_3)_2]_2$ (M = Mn, Fe, Co) in the vapor.[11] A further comparison may be drawn with the variable-temperature solution study of the cobalt alkoxide $[Co(OCPh_3)_2]_2$.[26] Heating a solution of this compound to ca. 75 °C results in the coalescence of the bridging and terminal signals. The activation energy for this process is about 13–14 kcal mol^{-1}. It is not known with certainty that this molecule dissociates like **1**. It is possible, however, that the bridging and terminal peaks may coalesce without the necessity of the dissociation of $[Co(OCPh_3)_2]_2$ into monomers. The substantially higher energy seen for the alkoxide is in agreement with stronger metal–oxygen bonding and with the less crowded nature of this complex owing to the presence of only one organo substituent on the atom attached to the metal.

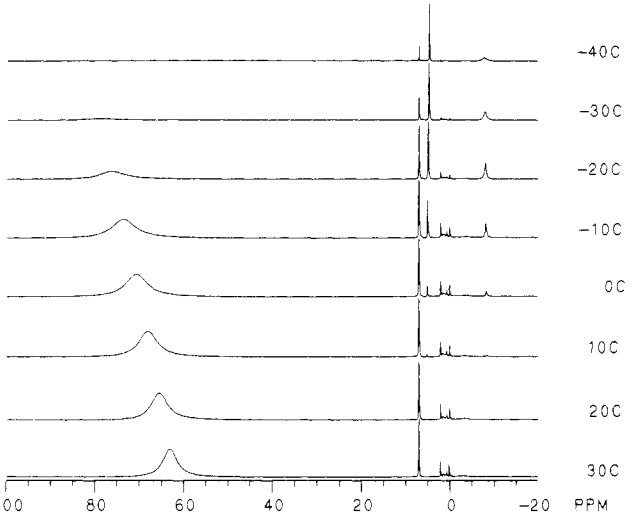

Figure 4. ^1H NMR spectra recorded in C_7D_8 for the monomer–dimer equilibrium of **1**.

Structures. The crystal structures of **1–3** are rare examples of the coordination number 3 for iron. Until recently, only two

(24) Fröhlich, H.-O.; Romhild, W. *Z. Chem.* **1980**, *20*, 154.
(25) Signer, R. *Justus Liebigs Ann. Chem.* **1930**, *478*, 246.
(26) Sigel, G. A.; Bartlett, R. A.; Decker, D.; Olmstead, M. M.; Power, P. P. *Inorg. Chem.* **1987**, *26*, 1773.

such examples had been authenticated structurally: the iron(III) species $Fe[N(SiMe_3)_2]_3$ (**6**) (Fe–N = 1.917 (4) Å)[27] and the iron(II) silyl complex $[FeCl\{Si(SiMe_3)_3\}_2][NEt_4]$.[28] Data for **1** and **3** and for related metal(II) amides involving Mn, Co, and Ni are provided in Table IV. Vapor electron diffraction data for $M[N(SiMe_3)_2]_2$ (M = Mn, Fe, Co) are also given.[11] Since **1** dissociates to monomers in solution, the structural data for the crystalline, monomeric, two-coordinate Fe(II) amides **4** and **5** are also listed in Table IV. Inspection of these data show that there are relatively minor variations in the terminal Fe–N bond lengths in most of the compounds. For example, the Fe–N distance in **1** is only marginally (0.01–0.02 Å) longer than the values seen in **3**, **5**, and **6**. The Fe–N distances in the less sterically crowded monomer, **4**, are shorter than those seen in the other two-coordinate iron species (see also ref 14), but within two standard deviations of the other Fe–N lengths. These data imply that the formation of bridges in the case of **1** has only a minor effect on the terminal Fe–N distances. In addition, they support the view that the bridging in **1** is quite weak. The Fe–N distance observed in the crowded molecule $Fe[N(SiMe_3)_2]_3$[27] (**6**) is presumably a compromise between the opposing effects of the smaller size of Fe^{3+} and three large $N(SiMe_3)_2$ substituents. The relatively constant values for the terminal Fe–N bond lengths observed in the crystal structures of **1**–**6** are in sharp contrast to the value of 1.84 Å quoted for the vapor-phase structure as determined by electron diffraction.[11] In this case, however, it was noted that the M–N (M = Mn, Fe, Co) values had low accuracy owing to their strong correlation with the Si–C bond distance. When both the Si–C and Si–N parameters were constrained, a slightly longer Fe–N distance of 1.85 (1) Å was obtained, but this distance is a good deal short of the >1.9 Å seen in the crystal structures. An alternative explanation for the short Fe–N bond length involves the Fe^{2+} center being in the low-spin configuration. This is unlikely because of the low overall crystal field strength of the two amide ions. In addition, the iron(2+) amides that are known to be two-coordinate in the solid state are all high spin.[10,12,14]

The bonding in **1** and **2** clearly shows the different effects of the $SiMe_3$ and phenyl substituents on the bonding in the metal amides. The Fe–N bonds in **2** average 0.03–0.05 Å shorter than those in **1**. The shortening is most noticeable in the case of the bridge bonds. These differences are probably a result of the lower basicity and greater size of the $-N(SiMe_3)_2$ ligand in comparison to $-NPh_2$. The lower amide basicity in **1** may arise because of the greater ionic character of the N–Si bond, which results in the lone pair being strongly attracted by silicon centers. It is tempting to regard the low angle between the Fe_2N_2 core and the N plane in terminal $-NPh_2$ as indicative of some Fe–N π-bonding. However, SCF–MO calculations on the hypothetical species $Mn(NH_2)_2$ indicate that the Mn–N interaction is primarily ionic.[11] Presently available data appear to support this picture. The terminal Fe–N distances in compounds **1** and **3**–**5** are only marginally shorter than those in $Fe[NMesBMes_2]_2$ (Fe–N = 1.938 (2) Å).[14] The latter compound is expected to have little Fe–N π-bonding owing to the strong N–B π-interaction. In addition, the slightly longer Fe–N bond in this compound could be accounted for in terms of the large size of the $-NMesBMes_2$ group.

The stability of the complex $Fe[N(SiMe_3)_2]_2(THF)$ (**3**) can be gauged from the fact that it maintains its integrity through several distillations under reduced pressure. As already noted, its Fe–N distance of 1.916 (5) Å is very similar to those observed in **1**, **4**, and **5**. Its structure resembles that of $Mn[N(SiMe_3)_2]_2(THF)$ (Mn–N = 1.99 (2) Å, Mn–O = 2.16 (2) Å), which was briefly described in a review.[5] The wide N–Fe–N angle 144.0 (3)°, which reflects the large size of the $-N(SiMe_3)_2$ ligand relative to THF, is similar to those reported for the Mn–N compound (145 and 150°). The complexation of only one THF is also of significance from the point of view of a comparison with $[Co(OCPh_3)_2]_2$.[26] The latter species complexes two THF's to give $[Co(OCPh_3)_2(THF)_2]$,[26] indicating that $-N(SiMe_3)_2$ is more crowding than $-OCPh_3$. This is, of course, in agreement with the conclusions of the ^1H NMR data discussed earlier. Other adducts of **1** with a variety of ligands can also form, and these along with the chemistry of **1** will be reported in the near future.

Acknowledgment. We thank the donors of the Petroleum Research Fund, administered by the American Chemical Society, for financial support.

Supplementary Material Available: Table S1, giving data for the calculation of the association energies of **1**, and Tables S2–S19, giving complete structural parameters and refinement data, atom coordinates, bond distances and angles, hydrogen coordinates, and anisotropic thermal parameters (14 pages); listings of structure factors (43 pages). Ordering information is given on any current masthead page.

(27) Bradley, D. C.; Hursthouse, M. B.; Rodesiler, P. F. *J. Chem. Soc., Chem. Commun.* **1969**, 14. Hursthouse, M. B.; Rodesiler, P. F. *J. Chem. Soc., Dalton Trans.* **1972**, 2100.
(28) Roddick, D. M.; Tilley, T. D.; Rheingold, A. L.; Geib, S. J. *J. Am. Chem. Soc.* **1987**, *109*, 945.